

Tailoring switching properties of dipolar species in ferroelectric liquid crystal with ZnO nanoparticles

This article has been downloaded from IOPscience. Please scroll down to see the full text article.

2009 J. Phys. D: Appl. Phys. 42 125413

(<http://iopscience.iop.org/0022-3727/42/12/125413>)

[The Table of Contents](#) and [more related content](#) is available

Download details:

IP Address: 140.113.159.62

The article was downloaded on 02/07/2009 at 11:42

Please note that [terms and conditions apply](#).

Tailoring switching properties of dipolar species in ferroelectric liquid crystal with ZnO nanoparticles

Liu-Shiaun Li and Jung Y Huang¹

Department of Photonics and Institute of Electro-Optical Engineering, Chiao Tung University, 1001 Ta Hsueh Road, Hsinchu, Taiwan 30010, Republic of China

E-mail: jyhuang@faculty.nctu.edu.tw

Received 3 March 2009, in final form 30 April 2009

Published 5 June 2009

Online at stacks.iop.org/JPhysD/42/125413

Abstract

The capacitance–voltage (C – V) characteristics of surface-stabilized ferroelectric liquid crystal (SSFLC) cells doped with zinc oxide nanocrystals (nc-ZnO) have been studied and fitted to the Preisach model to reveal the behaviours of dipolar species. To explain the experimental results, we propose a physical picture depicting an interaction of nc-ZnO dipole with surrounding SSFLC dipolar species. Our study shows that doping nc-ZnO into FLC not only increases the contrast ratio of the cells by 10 times but also enhances the dynamic polarization of the beneficial dipolar species while minimizing the polarization response of the species with counter effects.

(Some figures in this article are in colour only in the electronic version)

Surface-stabilized ferroelectric liquid crystal (SSFLC) devices were first proposed by Clark and Lagerwall to yield attractive properties, including microsecond response time, bistability and wide viewing angle [1]. However, to meet the industrial application criteria, further improvements in the properties of ferroelectric liquid crystal (FLC) to yield better contrast, higher stability of smectic layer structure and lower driving voltage are required. Modifying an existing FLC material by doping with appropriate nanoparticles could produce new FLC by blending instead of synthesizing new mesogenic molecules and has therefore attracted significant interest recently [2–5]. Insight into the interaction between nanoparticle and FLC species is indispensable for a better design of the blending scheme. In our previous investigation [6], we applied time-resolved Fourier transform infrared absorption spectroscopy to discover an nc-ZnO induced molecular binding effect on the FLC species. Although capacitance–voltage (C – V) characteristics of the SSFLC cells with multiple FLC dipolar species were also reported to reveal the effect of nc-ZnO doping, the interaction between nc-ZnO and FLC dipolar species at various driving frequencies had not been characterized in detail. After conducting more measurements, we reported in this

paper that nc-ZnO doping can indeed improve the electro-optical response of the SSFLC by enhancing the dynamic polarization of the beneficial dipolar species while minimizing the polarization of the species with counter effects.

Colloidal zinc oxide nanoparticles were synthesized with a sol–gel process [6–8], producing nc-ZnO with an averaged diameter of 3.2 nm [6]. The commercial room-temperature FLC mixture FELIX 017/100 FLC (from Clariant, Frankfurt, Germany) with spontaneous polarization of 47 nC cm^{-2} at 25°C exhibits a thermotropic transition sequence of $\text{Cr} \xrightarrow{-28^\circ\text{C}} \text{SmC}^* \xrightarrow{73^\circ\text{C}} \text{SmA}^* \xrightarrow{77^\circ\text{C}} \text{N}^* \xrightarrow{85^\circ\text{C}} \text{Iso}$. To prepare a doped FLC material, an appropriate amount of ZnO nano powder was added into the FLC and then homogenized with an ultrasonic cleaner at 85°C for 40 min. The substrates of each SSFLC cell are indium tin oxide (ITO)-coated glass plates $12 \text{ mm} \times 15 \text{ mm}$ in dimension, which were coated with SE7492 polyimide (PI) (from Nissan Chemical) and rubbed unidirectionally to produce a uniform FLC alignment. We assembled the SSFLC cells with two anti-parallel rubbed substrates and maintained the cell gap with $2 \mu\text{m}$ diameter silica balls dispersed in a UV-curable gel NOA65. The resulting nc-ZnO doped FLC was filled into a test cell in its isotropic phase and then cooled slowly to 35°C to form a stable single SmC^* domain. The

¹ Author to whom any correspondence should be addressed.

C - V measurements of the SSFLC cells were carried out at 25 °C with a computer-controlled HP4284A LCR meter, which provides a bias voltage range of ± 35 V with a sinusoidal wave of 1.0 V in the frequency range 20 Hz–1 MHz. We characterized each empty cell with C - V measurement to verify each empty cell to have a voltage-independent capacitance of 717 ± 35 pF at 1 kHz.

Note that ZnO possesses a wurtzite structure that allows the ZnO nanoparticles of $2R_0 = 3.2$ nm to carry a permanent dipole moment of $\mu_{\text{ZnO}} = 50$ D [9, 10]. Therefore, before conducting our investigation, we are interested in estimating the dipole–dipole interaction energy $V = \mu_{\text{ZnO}}\mu_{\text{CO}}(1 - 3 \cos^2 \theta)/(4\pi \epsilon_0 r^3)$ [11] between nc-ZnO and one of the surrounding dipolar species μ_{CO} . Because the potential energy for the dipole–dipole interaction depends on their relative orientations θ , the molecules exert forces on one another and do not rotate completely freely. Thus, the lower energy orientations are favoured so there is a non-zero interaction between rotating dipoles. In our case, the nc-ZnO particles being nano-size objects behave like a molecular dopant in the SSFLC. At a uniform doping concentration of 1 wt%, one ZnO nanoparticle is surrounded by about $n_{\text{FLC}} = 15\,000$ molecules within a sphere of $R_{\text{max}} = 14$ nm centred at the nc-ZnO. The thermal average of the dipole–dipole interaction energy per unit volume between nc-ZnO and surrounding FLC molecules gives [11, 12]

$$U_a^{\text{ZnO-FLC}} = -\frac{2\mu_{\text{CO}}^2\mu_{\text{ZnO}}^2n_{\text{FLC}}N_{\text{ZnO}}}{3(4\pi\epsilon_0)^2k_{\text{B}}TR_0^3R_{\text{max}}^3}. \quad (1)$$

We obtained $U_a^{\text{ZnO-FLC}} \approx 1000 \text{ J m}^{-3}$ by using $N_{\text{ZnO}} = 1.4 \times 10^{23} \text{ m}^{-3}$, $\mu_{\text{CO}} = 1.5$ D, $\mu_{\text{ZnO}} = 50$ D, $R_0 = 1.6$ nm, and $k_{\text{B}}T = 4 \times 10^{-21}$ J. This interaction has an alignment effect similar to what FLC molecules experience within a distance of 100 nm from an alignment surface with an anchoring strength of $1 \times 10^{-4} \text{ J m}^{-2}$ and produce an observable effect in our SSFLC cells.

To probe the azimuthal alignment of FLC, we inserted a SSFLC cell into an optical setup involving a crossed polarizer–analyzer and oriented the rubbing direction of the test cell to the transmission axis of the input polarizer. The optical transmittance of the test cells was measured as a function of the azimuthal angle of the rubbing direction. The resulting azimuthal patterns of the optical transmittance of an undoped SSFLC cell (filled squares) and that doped with nc-ZnO (filled triangles) are presented in figure 1. Compared with the undoped cell, nc-ZnO doping reduces the light leakage of the dark state by 9 times while improving the optical throughput of the bright states by 1.2 times. This leads to an increase in the contrast ratio by 10 times, suggesting that the alignment of the FLC molecules is improved effectively with the doping.

We investigated the field-induced switching properties of nc-ZnO doped SSFLC by invoking an equivalent electronic circuit model of SSFLC depicted in figure 2(a) [13]. In our SSFLC cells, the thickness and the dielectric constant of PI were determined to be 150 nm and $\epsilon_{\text{PI}} = 3.8$, respectively, leading to a capacitance of $C_{\text{PI}} = 200$ nF for the PI layer. The electrical resistance R_{PI} of the PI was measured to be

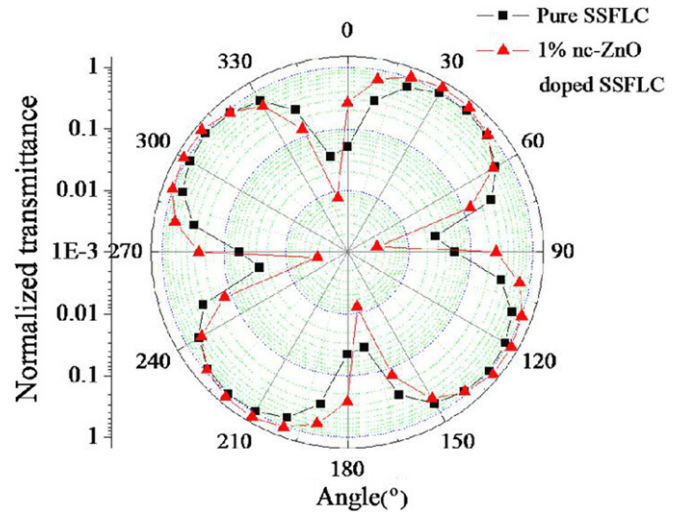


Figure 1. Azimuthal patterns of the optical transmittance of an undoped SSFLC cell (filled squares) and that doped with nc-ZnO (filled triangles).

about $10^{10} \Omega$. Thus, as the cell is driven above 100 Hz, the R_{PI} is negligible in the circuit model [13]. With the C_{PI} much larger than the cell capacitance, C_{cell} can be approximated to be C_{FLC} . The C - V hysteresis curves of our SSFLC cells with pure FLC and nc-ZnO doped FLC are presented in figures 2(b) and (c), respectively. At the four different frequencies, the peak capacitances of the nc-ZnO doped SSFLC cell are always larger than that of the pure FLC. The bias voltages at the peak capacitances of the doped SSFLC cell are closer to 0 V than that of the pure FLC. The peak capacitance was found to decrease with increasing driving frequency, indicating that more and more dipolar species are unable to respond to the driving field.

To more quantitatively reveal the doping with nc-ZnO, the Preisach model was invoked to derive $C(V_{\text{ex}}) = C_{\text{const}} + A \cdot [dP(V_{\text{ex}})/dV]$ and $P(V_{\text{ex}}) = P_{\text{S}} \cdot \tanh[\delta \cdot (V \pm V_{\text{C}}^{\mp})]$ [14–17]. For the case of FLC with multiple dipolar species [6], the cell capacitance can then be expressed as

$$C_{\text{cell}}(V_{\text{ex}}) = C_{\text{const}} + \sum_{i=1}^n \frac{P_{\text{si}} \cdot \delta_i}{\cosh^2[\delta_i \cdot (V_{\text{ex}} \pm V_{\text{Ci}}^{\mp})]} \cdot A, \quad (2)$$

where C_{const} denotes the voltage-independent part of the capacitance of FLC; A is the cell area; P is the polarization and V_{ex} is the driving voltage. P_{si} in equation (2) represents the spontaneous polarization as all dipoles of the i th species are fully aligned to an external field. V_{Ci}^{\pm} is the coercive voltage at which the electric polarization of the i th species vanishes during switching from one orientation to the other orientation [18, 19]. $\delta_i = \log\{[1 + (P_{\text{r}}/P_{\text{s}})_i]/[1 - (P_{\text{r}}/P_{\text{s}})_i]\}/V_{\text{Ci}}$ is a species-related constant with P_{r} and P_{s} denoting the remanent and spontaneous polarizations, respectively. The (\pm) sign refers to an increasing/decreasing V_{ex} .

As shown in figures 3(a) and (b), we found that four dipolar species ($n = 4$) are involved in the SSFLC. By doping with nc-ZnO, the peak capacitance contributed by species 1 is increased while capacitances from species 2, 3 and 4 are reduced. The doping also causes P_{s} to behave in a similar

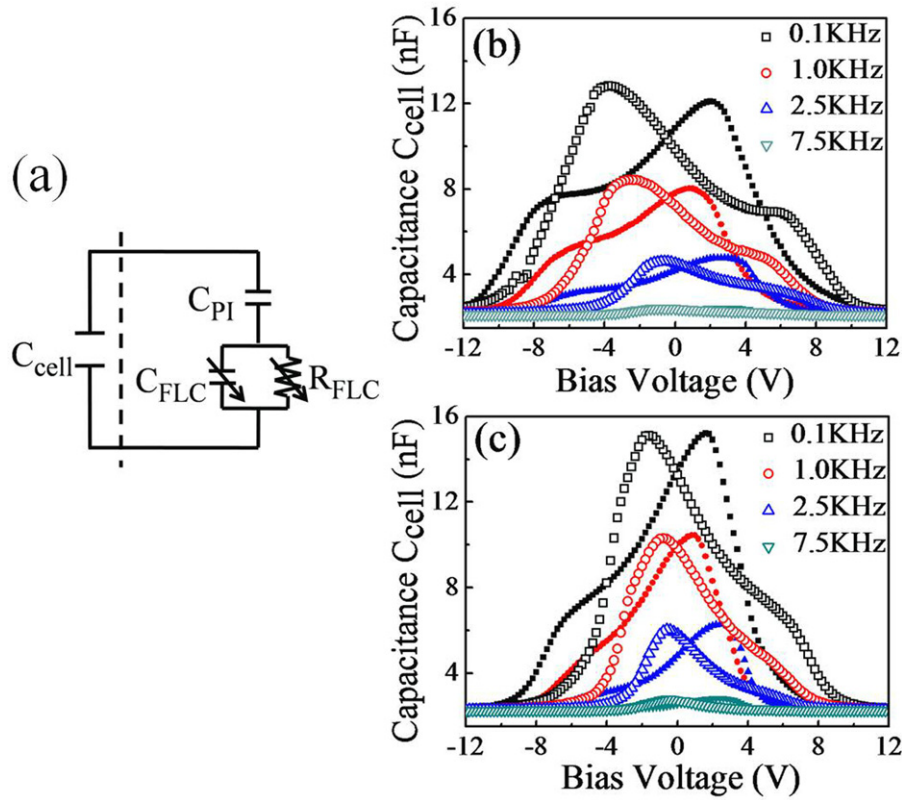


Figure 2. (a) The equivalent electronic circuit model of the SSFLC used in this study. The capacitance–voltage (C – V) characteristics of (b) an undoped SSFLC cell and (c) a doped SSFLC cell with 1% nc-ZnO measured at four different frequencies. The filled and the open symbols are the data obtained with a negative-to-positive and a positive-to-negative voltage sweep, respectively.

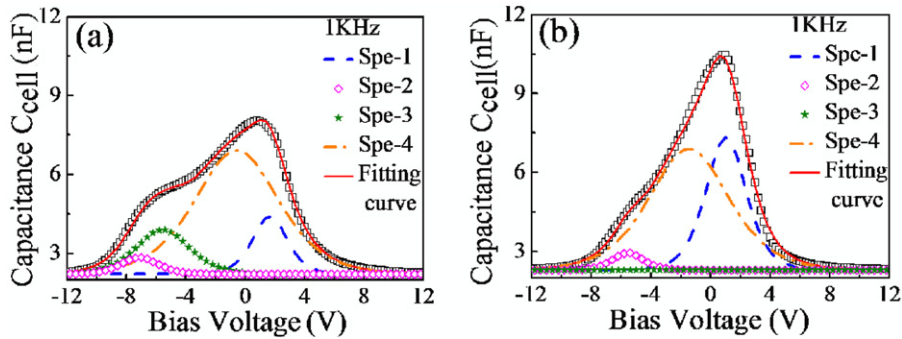


Figure 3. The C – V characteristics (open squares) at 1 kHz and the corresponding fitting curves (solid lines) and the contributions from the four dipolar species in a SSFLC cell (a) without and (b) with nc-ZnO doping.

way. The P_s from species 1 is increased by doping and makes the peak capacitance of the doped SSFLC cell higher than the undoped cell. ZnO nanocrystal doping also decreases V_c of species 1 by 1.2 V, while increasing V_c of species 2 and 4 by 1.5 V and 0.5 V, respectively. Based on the C – V analysis presented in figures 3(a) and (b), we concluded that V_c at the peak capacitances of the SSFLC cells is mainly determined by species 1, which is true no matter whether SSFLC is doped by nc-ZnO or not.

The electrical properties of a ferroelectric material are also conveniently presented in the polarization–voltage (P – V) curve. We can convert the measured C – V characteristics to the P – V curves by using the Preisach model [14–17]. In figure 4, the summed electrical polarization from the four species in an

undoped SSFLC cell is shown with the dashed curves while the solid lines are for an nc-ZnO doped SSFLC. Note that under the same bias voltage, the dipolar species with larger polarization take less time to reach the direction of the applied field [14, 15]. We found that P_s in the undoped and doped SSFLC cells is identical when the applied voltage is larger than 8 V. But when the applied voltage lies between -8 and 8 V, the nc-ZnO doped FLC does yield larger polarization. The improved polarization is mainly contributed by species 1, which exhibits a behaviour of increased polarization and reduced coercive voltage by doping, suggesting that doping with nc-ZnO does effectively improve the dynamic polarization response of species 1.

One of the major advantages of SSFLC is microsecond response time for true video rate applications. Therefore, it is

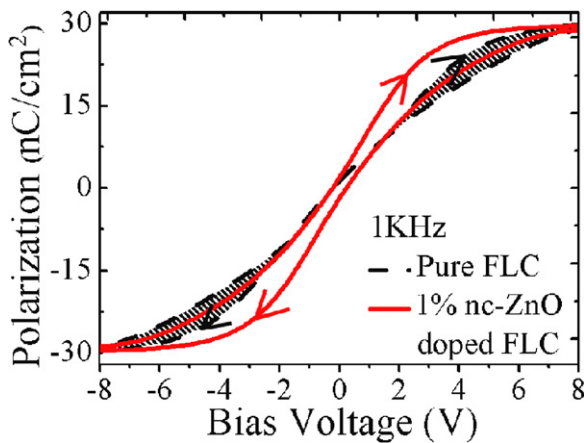


Figure 4. The polarization–voltage (P – V) characteristics at 1 kHz. The black dash and red solid lines indicate the data for pure SSFLC and 1% nc-ZnO doped SSFLC, respectively. The up arrows denote that the bias voltage is increased from -8 V to $+8$ V and the arrows pointing down for decreasing voltage from $+8$ V to -8 V.

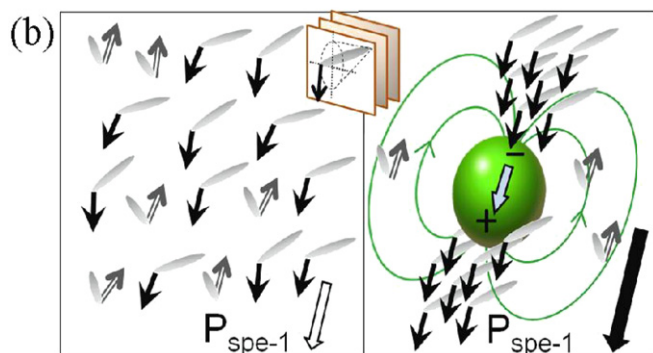
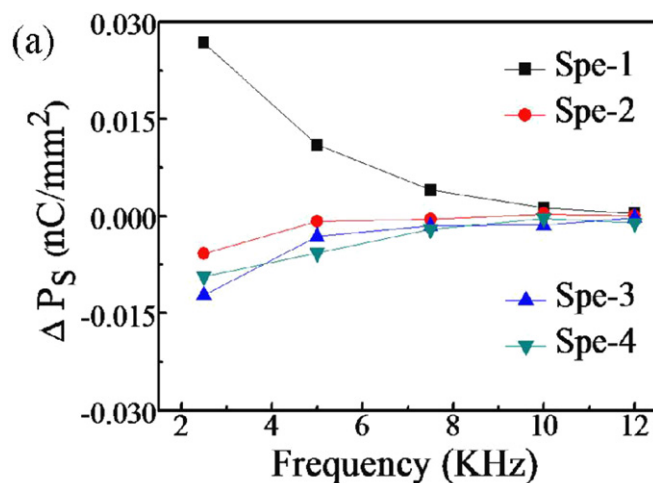


Figure 5. (a) The doping-induced spontaneous polarization changes (ΔP_s) in the four dipolar species in a SSFLC cell as a function of driving frequency. (b) Schematic drawing illustrating the dipolar interaction of species 1 in an undoped SSFLC cell (left) and the dipolar interaction of species 1 with nc-ZnO in a doped SSFLC cell (right). The inset figure shows the smectic layer structure of SSFLC and $P_{\text{spe-1}}$ denotes the spontaneous polarization of species 1.

interesting to investigate how P_s of the four dipolar species varies at high driving frequencies. Figure 5(a) shows that nc-ZnO doping results in an increase in P_s of species 1 while that from the remaining three species are diminished; this

supports the notion that doping with nc-ZnO can enhance the dynamic polarization of the beneficial dipolar species while it minimizes the polarization response of the species with counter effects. The doping-induced spontaneous polarization change (ΔP_s) of the four species decays with driving frequency. Figure 5(b) presents a schematic drawing illustrating an idea about the dipolar interaction of species 1 in an undoped and a doped SSFLC cell. Dipoles associated with species 1 could adjust their spatial distribution and likely aggregate on those regions near the north and south poles of the nc-ZnO, and accordingly align in the same direction with the nc-ZnO dipole. The number of the dipolar species 1 lying on the equatorial plane of the nc-ZnO becomes smaller. P_s from species 1 can therefore be increased by nc-ZnO doping.

In summary, doping FLC with nc-ZnO not only increases the contrast ratio by 10 times, but also improves the electro-optical response by increasing the spontaneous polarization and reducing the coercive voltage of the beneficial dipolar species while minimizing the polarization of the species with counter effects. We also show that a ZnO nanoparticle can interact with its surrounding FLC dipolar species and tie the FLC species together to respond to an external driving field in more unison. Thus, nc-ZnO doping into FLC could become a simple yet effective way to tailor the field-induced switching properties of an existing FLC.

Acknowledgments

This research was supported by the National Science Council of the Republic of China under grant NSC97-2112-M009-006-MY3 and Taiwan TFT LCD Association. Fruitful discussions with Professor Wha-Tzong Whang and Dr Chin-Hsien Hung of the Department of Materials Science and Engineering of Chiao Tung University are also deeply appreciated.

References

- [1] Clark N A and Lagerwall S T 1980 *Appl. Phys. Lett.* **36** 899
- [2] Shiraiishi Y, Toshima N, Maeda K, Yoshikawa H, Xu J and Kobayashi S 2002 *Appl. Phys. Lett.* **81** 2845
- [3] Kaur S, Singh S P, Biradar A M, Choudhary A and Sreenivas K 2007 *Appl. Phys. Lett.* **91** 023120
- [4] Reznikov Y, Buchnev O, Tereshchenko O, Reshetnyak V, Glushchenko A and West J 2003 *Appl. Phys. Lett.* **82** 1917
- [5] Li F, Buchnev O, Cheon C I, Glushchenko A, Reshetnyak V, Reznikov Y, Sluckin T J and West J L 2006 *Phys. Rev. Lett.* **97** 147801
- [6] Huang J Y, Li L S and Chen M C 2008 *J. Phys. Chem. C* **112** 5410
- [7] Goyal D J, Agashe C, Takwale M G, Bhide V G, Mahamuni S and Kulkarni S K 1993 *J. Mater. Res.* **8** 1052
- [8] Meulenkamp E A 1998 *J. Phys. Chem. B* **102** 5566
- [9] Shim M and Guyot-Sionnest P 1999 *J. Chem. Phys.* **111** 6955
- [10] Nann T and Schneider J 2004 *Chem. Phys. Lett.* **384** 150
- [11] Keesom W H 1921 *Phys. Z.* **22** 129
- [12] Magnasco V, Battezzati M, Rapallo A and Costa C 2006 *Chem. Phys. Lett.* **428** 231
- [13] Blinov L M, Pozhidaev E P, Podgornov F V, Pikin S A, Palto S P, Sinha A, Yasuda A, Hashimoto S and Haase W 2002 *Phys. Rev. E* **66** 021701
- [14] Miller S L, Nasby R D, Schwank J R, Rodgers M S and Dressendorfer P V 1990 *J. Appl. Phys.* **68** 6463

- [15] Miller S L, Schwank J R, Nasby R D and Rodgers M S 1991 *J. Appl. Phys.* **70** 2849
- [16] Yang P, Carroll D L, Ballato J and Schwartz R W 2002 *Appl. Phys. Lett.* **81** 4583
- [17] Rahman M, Kundu S K, Chaudhuri B K and Yoshizawa A 2005 *J. Appl. Phys.* **98** 024114
- [18] Blinov L M and Chigrinov V G 1993 *Electrooptic Effects in Liquid Crystal Materials* (New York: Springer) p 387
- [19] Demus D, Goodby J, Gray G W, Spiess H-W and Vill V 1998 *Handbook of Liquid Crystals Vol 2B: Low Molecular Weight Liquid Crystals II* (New York: Wiley) p 522